AD-A115 862 GENERAL ELECTRIC CO SCHENECTADY N Y F/G 20/13
NONLINEAR THERMOELASTIC EFFECTS IN SURFACE MECHANICS.(U)
1980 J M PITKIN N00014-80-C-0253
UNCLASSIFIED NL

final report for Contract N00014-80-C-0253

NONLINEAR THERMOELASTIC EFFECTS IN SURFACE MECHANICS

J.M. Pitkin
General Electric Company
Schenectady, New York

ABSTRACT

The nonlinear thermoelastic equations are examined, considering large deformations and temperature-dependent material parameters. Emphasis is on high-speed sliding contacts, wherein high temperatures localize near the contact surface, contributing to significance there of coupling terms neglected in elementary theory.

NOMENCLATURE

- $\mathbf{A}$ = Coefficient matrices for governing equations
- A_k = Combinations of elastic parameters, Eqs. (20); alternatively, complex coefficients defined following Eqs. (10), ($k = 1, \ldots, 5$)
- a_n = Complex coefficients of material inhomogeneity, Eqs. (10), $n = 1,2$
- a = Half contact width, m
- $\underset{\sim}{B}$ = Vector, nonhomogeneous part of difference equations
- B_j = Boussinesq-Papkovitch functions, $j = 0,1,2$
- c_E = Specific heat at constant deformation (or at constant volume for subscript v), J/(kg·K)
- c_o = Value of c_E at reference temperature T_o
- E_{ij} = Lagrangian strain components
- E = Young's modulus, Pa
- f = Thermal dependence of c_E, c_E/c_o; alternatively, scalar function of $\underset{\sim}{v}$
- g = Thermal dependence of k, k/k_o
- $\underset{\sim}{g}$ = Gradient of $f(\underset{\sim}{U})$, $\partial f/\partial \underset{\sim}{U}$
- $\underset{\sim}{H}$ = Hessian matrix of $f(\underset{\sim}{U})$, Eq. (15)
- h_k = Finite difference grid spacing for ξ_k, $k = 1,2$
- k = Thermal conductivity, W/(m·K)
- k_o = Value of k at reference temperature T_o
- ℓ = 2a, contact width, m
- M = Mechanical equivalent of heat, 1.0 N·m/J
- P_o = Péclet Number, defined following Eq. (7)
- P_{nij} = Traction coefficients, Eqs. (20), Pa
- p = Contact pressure, $p(\xi_1)$, Pa
- Q = Heat flux, Lagrangian description, W
- S = Nonhomogeneous part of complex traction boundary condition, Eqs. (10); alternatively, quadratic scalar function of $\underset{\sim}{U}$, Eq. (18)
- T = Temperature, °C
- T_o = Reference temperature, 293 K (528°R), unless indicated otherwise
- T' = Dimensionless temperature, $(T - T_o)/T_o$
- t = Time, s
- $\underset{\sim}{U}$ = Solution vector
- U_k = Dimensionless displacement components u_k/ℓ
- u_k = Displacement components, $k = 1,2$
- V = Speed of contact sliding, m/s
- v_{ijk} = Generalized wave speeds, Eqs. (19), m/s
- w = Generalized analytic function, $w(z, \bar{z})$
- X_k = Space coordinates, Lagrangian description, m
- z = Complex variable, $\zeta_1 + i\zeta_1$
- α = Coefficient of linear thermal expansion, 1/K
- β = Coefficient of bulk thermal expansion = $(3\lambda + 2\mu)\alpha$, Pa/K
- $\dot{\epsilon}_{kk}$ = Dilatation rate, conventional (small strain) notation, 1/s
- ζ_k = Transformed space variables, $k = 1,2$
- η = Boundary layer (stretched) thickness coordinate
- λ, μ = Lamé parameters, Pa
- μ_F = Friction coefficient
- ν = Poisson's ratio
- ν_k = Third order elastic parameters, notation of Toupin and Bernstein, $k = 1,2,3$
- ξ_k = Dimensionless space variables, X_k/ℓ, $k = 1,2$
- ρ_o = Reference density, kg/m^3
- Σ_{ij} = Components of Piola-Kirchhoff Stress, First Kind, Pa
- Φ, Ψ = Analytic functions
- Φ_p, Ψ_p = Generalized analytic functions
- Ω_{1k} = Generalized Cauchy kernels, Eq. (11)
- ω_{1k} = Exponential factor for Ω_{1k}
- ω_i = Relaxation factors, Eq. (14)

INTRODUCTION

Generation of large amounts of heat near the surface of a thermoelastic body subjected to fast-moving contact loads is a generally recognized occurrence. Important in such a situation is the thermally-induced deformation, affecting the contact stress distribution which, in turn, affects the heat input. Stabilization by limitation of temperatures and deformations to steady-state values follows only if deformations are balanced by wear [1,2] leading to maximum possible contact after "wearing-in."

Simple contact configurations permit temperature measurements by either noncontacting infrared devices or thermocouples embedded without disturbing temperature flow [1-3]; surface deformations are inferred from laser/photocell system measurements of surface clearances [3]. Such measurements, however, are insufficient for complete descriptions of temperatures and deformations and must be supplemented by analysis. Accurate analytical predictions aid interpretation of experimental results and provide guidance for situations wherein measurements are not feasible.

Conventional thermoelastic analyses (linear, uncoupled thermal and elastic effects) often give temperature predictions at variance with results of wear tests. Under examination herein is the significance of thermoelastic nonlinearities, viewed toward explaining such discrepancies. The following observations are pertinent in this respect:

1. Apparent temperature jumps across the contact surface and other anomalies are predicted in extrapolations, by conventional theory, from near-surface embedded thermocouple readings [3].

2. Neglect of thermoelastic coupling is usually based on considerations that tacitly assume only moderate heat generation [4]. Temperatures of several hundred degrees generated in high-speed sliding, however, can render the coupling terms significant.

3. Usual treatments of thermoelastic coupling consider only dilatational effects. Significant temperature buildups have been generated experimentally, however, under repeated cycling of elastic deviatoric strains [5].

4. Variation of thermal parameters with temperature can significantly affect heat conduction in sliding contacts, as analysis demonstrates [6].

The reality of irreversible, often large, deformations and/or strains accompanied by heat generation under inelastic conditions led long ago [7] to recognition of the importance therein of thermomechanical coupling. In thermoelasticity, however, a typical argument [4] considers only the simplest coupling, involving a dilatational term in the heat conduction equation with magnitude governed by the factor $3(\beta\alpha T_0/\rho c_v)(\dot{\epsilon}_{kk}/3\alpha\dot{T})$. Using isothermal values of β, α, c_v for a typical steel and for aluminum and 366 K (660°R) for T_0, the factor $3(\beta\alpha T_0/\rho c_v)$ is evaluated as 0.01793 and 0.03714, respectively; it is concluded that coupling is negligible if $(\dot{\epsilon}_{kk}/3\alpha\dot{T}) \ll 20$ and this is assumed to be the case. On the other hand, high-temperature values [8-10] of β, α, c_v for a typical steel at 665°C (1230°F) - an attainable dry sliding surface temperature [6] - give 0.1576 for $3(\beta\alpha T_0/\rho c_v)$. Thus, even if $(\dot{\epsilon}_{kk}/3\alpha\dot{T})$ is only of order 1.0 the coupling term in this case has an order ~ 16% of the basic term $\rho c_v\dot{T}$. The apparent importance of this simplest coupling term suggests examining the significance of additional relevant coupling terms, as well.

THEORY

Analytical Model

Evidence that high-speed sliding contact situations produce temperatures and material degradation localized mainly near the contact surface permits consideration of a semi-infinite solid with contact loads moving along a plane boundary. Applying the plane boundary idealization to problems involving curved surfaces gives an error in the governing equations of order $P_0^{-1/2}R^{-1}$, with P_0 the Pèclet Number and R the ratio of the surface radius of curvature to a typical length (e.g., the surface contact width). In addition, only a two-dimensional model is needed because high-speed sliding leads, essentially, to suppression of heat flow in the surface direction perpendicular to sliding [11]. The model utilized is a plane strain one, applicable to a large contact length in the latter direction.

Figure 1 shows the undeformed solid, subjected to mechanical loads $p(X_1)$ and $\mu_f p(X_1)$ over the surface region $0 \le X_1 \le 2a$, $X_2 = 0$, $|X_3| < \infty$, moving with constant speed V relative to the bulk solid; the latter load is a frictional force per unit of material thickness in the X_3-direction. Coordinate system X_k' $(k = 1,2,3)$ is fixed with respect to the material, whereas system X_k is fixed with respect to the loading. The material is considered to be isotropic, free of body forces, and to have temperature-dependent material parameters. In addition, the friction coefficient is generally a nonlinear function of velocity, linear asymptotically at high sliding speeds. Considering steady-state, high-speed sliding fixes the friction coefficient and rules out self-sustained ("chattering") oscillations [12]. The surface

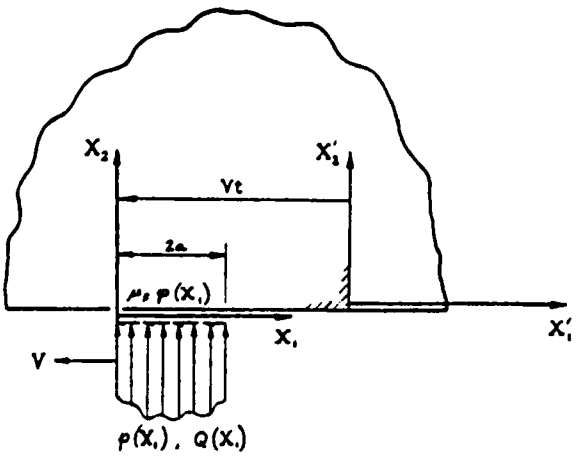

Figure 1 Schematic Diagram of the Half-Space Subjected to Mechanical and Thermal Loading

frictional force generates dissipative energy that produces a heat source with flux $Q(X_1) = V\mu_f p(X_1)/M$; the remainder of the surface is assumed insulated. Pressure $p(X_1)$ is considered to be the force on the deformed surface per unit area of undeformed surface, since the deformed shape is not known a priori. Thus, the applied loads are surface tractions related to Piola-Kirchhoff stresses of the First Kind Σ_{ij} [13-15]. Similarly, heat flux $Q(X_1)$ is that referred to the undeformed solid [13-15].

Governing Equations

With respect to reference frame X_k, convected with the surface loading according to $X_k = X_k' + \delta_{k1}Vt$, displacements and temperatures are quasi-stationary [6,11]. Thus, e.g., $u_k(X_1', X_2', t) = u_k(X_1 - Vt, X_2)$, so that

$$\left(\frac{\partial u_k}{\partial t}\right)_{\underset{\sim}{X}'} = \left(\frac{\partial u_k}{\partial t}\right)_{\underset{\sim}{X}} + \left(\frac{\partial \underset{\sim}{X}}{\partial t}\right)_{\underset{\sim}{X}'}\left(\frac{\partial u_k}{\partial \underset{\sim}{X}'}\right)_t = V\frac{\partial u_k}{\partial X_1}, \qquad (1)$$

etc. Hence, velocities and accelerations referred to material coordinates X_k' can be expressed entirely in terms of convected coordinate X_1, without explicit dependence on t. Application to the nonlinear thermoelastic equations referred to material coordinates X_k' [15] permits their expression in terms of the convected coordinates. The two momentum equations and the heat equation (after rearranging and nondimensionalizing) are then, respectively,

$$\left[1 - \left(\frac{v}{v_{111}}\right)^2\right]u_{1,11} + 2\left(\frac{v_{112}}{v_{111}}\right)^2 u_{1,12} + \left(\frac{v_{122}}{v_{111}}\right)^2 u_{1,22} + \left(\frac{v_{211}}{v_{111}}\right)^2 u_{2,11} + \left(\frac{v_{212}}{v_{111}}\right)^2 u_{2,12} + \left(\frac{v_{112}}{v_{111}}\right)^2 u_{2,22} - \left(\frac{v_{113}}{v_{111}}\right)^2 T'_{,1} - \left(\frac{v_{123}}{v_{111}}\right)^2 T'_{,2} = 0, \qquad (2)$$

$$\left(\frac{v_{211}}{v_{122}}\right)^2 U_{1,11} + \left(\frac{v_{212}}{v_{122}}\right)^2 U_{1,12} + \left(\frac{v_{112}}{v_{122}}\right)^2 U_{1,22} + \left[1 - \left(\frac{V}{v_{122}}\right)^2\right] U_{2,11} + 2\left(\frac{v_{211}}{v_{122}}\right)^2 U_{2,12} + \left(\frac{v_{222}}{v_{122}}\right)^2 U_{2,22} - \left(\frac{v_{213}}{v_{122}}\right)^2 T'_{,1} - \left(\frac{v_{223}}{v_{122}}\right)^2 T'_{,2} = 0, \quad (3)$$

$$\left(\frac{v_{311}}{v_T}\right)^2 U_{1,11} + \left(\frac{v_{312}}{v_T}\right)^2 U_{1,12} + \left(\frac{v_{411}}{v_T}\right)^2 U_{2,11} + \left(\frac{v_{412}}{v_T}\right)^2 U_{2,12} - \frac{1}{P_o}(T'_{,11} + T'_{,22}) - \frac{1}{P_o}\frac{g'}{g}\left[(T'_{,1})^2 + (T'_{,2})^2\right] + \left[\frac{f}{g} + \left(\frac{v_1}{v_T}\right)^2\right] T'_{,1} = 0, \quad (4)$$

Similarly, the boundary conditions take the form:

$$\Sigma_{22}(\xi_1, 0) = \left[P_{N11}U_{1,1} + P_{N22}U_{2,2} + P_{N12}U_{1,2} + P_{N21}U_{2,1} - \beta T'\right]_{\xi_2=0} = \left\{ \begin{array}{ll} -p(\xi_1), & 0 \le \xi_1 \le 1 \\ 0, & \xi_1 \notin [0,1] \end{array} \right\}, \quad (5)$$

$$\Sigma_{12}(\xi_1, 0) = \left[P_{S12}U_{1,2} + P_{S21}U_{2,1}\right]_{\xi_2=0} = \left\{ \begin{array}{ll} -\mu_F p(\xi_1), & 0 \le \xi_1 \le 1 \\ 0, & \xi_1 \notin [0,1] \end{array} \right\} \quad (6)$$

$$\frac{Q(\xi_1, 0)\ell}{k_o T_o} = \left[-g\frac{\partial T'}{\partial \xi_2}\right]_{\xi_2=0} = \left\{ \begin{array}{ll} P_o \dfrac{\mu_F p(\xi_1)}{\rho_o c_o T_o M}, & 0 \le \xi_1 \le 1 \\ 0, & \xi_1 \notin [0,1] \end{array} \right\}, \quad (7)$$

The coefficient terms v^2_{ijk}, P_{aik} appearing in Eqs. (2) - (6) are defined in Appendix A. In addition, dimensionless variables are $U_i = u_i/\ell$, $\xi_i = X_i/\ell$, $T' = (T - T_o)/T_o$, $f(T') = c_\ell(T')/c_o$, $g(T') = k(T')/k_o$, and abbreviations $(\,)_{,i} = \partial(\,)/\partial\xi_i$, $(\,)' = \partial(\,)/\partial T'$, $\ell = 2a$ apply. P_o is the Peclet Number, $V\ell\rho_o c_o/k_o$. The v^2_{ijk} all have dimensions of (velocity)^2 and v_{111}, v_{122} generalize the classical isothermal speeds of dilatational and shear waves, respectively.

Equations (2) - (4) differ from versions given previously [15] by allowing nonlinear (rather than simply linear) thermal variations of material parameters and by not neglecting T' compared to 1 in $[v^2_{111}, \ldots, v^2_{122}]$. However, dependence of thermal conductivity on strain [15], apparently never quantified experimentally, is neglected herein; further, the formulation allows for thermal dependence of third order elastic parameters ν_1, ν_2, ν_3, but lack of data forced use of only isothermal values in calculations.

Boundary Layer

Typical sliding contact speeds are much smaller than elastic wave speeds (e.g., by orders $\le 10^3$ vs. 10^8 in./sec for a typical steel), although they can yield large values of P_o. Thus, terms $[1 - (V/v_{111})^2]v^2_{111}$, etc., in momentum Eqs. (2), (3) can be considered to be of order O(1). Second derivatives of T' in the heat Eq. (4), on the other hand, are multiplied by P_o^{-1} which becomes small for large P_o. Hence, the term containing these derivatives becomes vanishingly small for large P_o, except in regions where $(T'_{,11} + T'_{,22})$ is $O(P_o)$. A first approximation to the solution calculated from this reduced differential order problem would be incapable of satisfying all specified thermal boundary conditions - in particular, Eq. (7) for $\xi_2 = 0$ vs. $T' \to 0$ as $\xi_2 \to \infty$. Analysis for the relevant characteristic curves clarifies this difficulty. The direction cosines n_1, n_2 of such a curve, related by $n_1^2 + n_2^2 = 1$, are found [16] from the relation $\det(A) = 0$, where A is the coefficient matrix for the vector $\{U_1\ U_2\ T'\}$ (transposed) in Eqs. (2) - (4), with $\partial/\partial\xi_i$ replaced by n_i $(i = 1, 2)$ [17]. The resulting algebraic equation is of fifth order (rather than sixth for the full problem) and has a real root $n_1 = 0$, giving curves $\xi_2 =$ constant generated by reduction in order of the heat equation. Vanishing temperatures prescribed (as Cauchy data) as $\xi_2 \to \infty$ should then define temperatures throughout the entire semi-infinite domain considered. The discrepancy so generated as $\xi_2 \to 0$ indicates the existence there of a boundary layer with $\partial T'/\partial\xi_2$ large.

The remaining quartic polynomial generated by $\det(A) = 0$ is presumed to not yield real roots (real characteristics) associated with elastic waves because of the smallness of V/v_{ijk} noted above. Another possibility, however, is that the momentum equations may fail to be elliptic for displacement gradient magnitudes exceeding certain bounds, as discussed recently [18,19] for isothermal plane finite elastostatics; treatment of thermal effects herein gives revised criteria. Consideration in what follows is restricted to the assumption, considered plausible for typical sliding situations, that displacement gradients and temperatures are only moderately large away from the contact; thus, the latter possibility fails to materialize. Then it is inferred [17] that the quartic has only imaginary roots, so only the above-mentioned boundary layer near $\xi_2 = 0$ occurs.

It can be shown that the boundary layer identified above has a thickness of order $O(P_o^{-1/2})$, corresponding to stretched thickness coordinate $\bar{\eta} = P_o^{1/2}\xi_2$. Thermoelastic behavior therein is controlled mainly by reduction of the heat equation from elliptic to parabolic type (having characteristics perpendicular to the contact surface rather than parallel to it as in the reduced case indicated above) and of the momentum equations to ordinary differential variety. Outside the boundary layer, temperatures are generally suppressed. In contrast, deformations are not so restricted, but even to first approximation are associated with a potential theory problem involving elliptic equations (see below). Significant boundary layer contributions to the deformations are exhibited only in higher approximations.

Detailed analysis [17] shows that the boundary layer is multi-structured and contains subregions smaller than $O(P_o^{-1/2})$ in which various approximations apply. For example, in small regions of size $O(P_o^{-1})$ about $\xi_1 = 0, 1$ no approximation is possible and the full elliptic equations (and potential solutions) govern. The boundary layer structure is shown schematically in Figure 2; some features are analogous to those for boundary layer flow past a flat plate [20,21].

Potential Theory Solutions

In theory, it is possible to obtain a solution by successive iteration between the heat and momentum equations, considering each in turn separately. This concept gives at least qualitative insight into the solution character. Treating the nonlinearities in the heat equation as a nonhomogeneous term $p^*(\xi_1, \xi_2)$ and removing thermal dependency of k (i.e., of g) by a transformation [6] $\varphi = \int_0^T g(T'')dT''$, due originally to

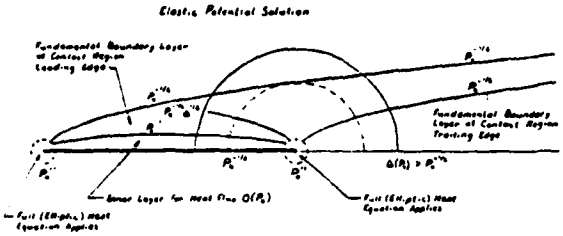

Figure 2 Schematic Representation of the Thermal Boundary Layer Structure

Kirchhoff [22], permits expression of the solution for φ as $\varphi = \varphi_A + \varphi_B$, where

$$\varphi_A(\xi_1,\xi_2,P_o) = \frac{1}{\pi}\int_o^1 e^{\frac{P_o}{2}(\xi_1-\xi_1')} \cdot K_o\left(\frac{P_o}{2}\sqrt{(\xi_1-\xi_1')^2+\xi_2^2}\right)Q^*(\xi_1')d\xi_1' \quad (8)$$

$$\varphi_B(\xi_1,\xi_2,P_o) = \frac{P_o}{2\pi}\int_{-\infty}^{\infty} e^{\frac{P_o}{2}(\xi_1-\xi_1')}\,d\xi_1' \int_o^{\infty} \cdot \left[K_o\left(\frac{P_o}{2}\sqrt{(\xi_1-\xi_1')^2+(\xi_2+\xi_2')^2}\right) + K_o\left(\frac{P_o}{2}\sqrt{(\xi_1-\xi_1')^2+(\xi_2-\xi_2')^2}\right)\right]p^*(\xi_1',\xi_2')d\xi_2' \quad (9)$$

and $K_o(\rho)$ is the modified Bessel function of the second kind, order zero. Equation (8) is equivalent to a previous result [22, p.269], obtained by superposition of heat sources, for only surface heat application by uniform heat flux over a strip area. Asymptotic considerations [17] show reduction as $P_o \to \infty$ of Eqs. (8), (9) to forms [6] having kernels $(\xi_1 - \xi_1')^{-1/2}\exp[-(\eta+\eta^*)^2/4(\xi_1-\xi_1')]$ with $\eta^* = 0$ for φ_A and $\eta^* = \pm\eta'$ for φ_B; integration for ξ_1 in φ_B then extends to 0, ξ_1, 1 for $\xi_1 < 0$, $0 \le \xi_1 \le 1$, $\xi_1 > 1$, respectively, and in φ_B always to ξ_1 (other ranges of ξ_1 yield exponentially small contributions).

Thermal dependence of the elastic material parameters can be mollified by transforming space variables in the momentum equations in analogy to that indicated above. Treating remaining nonlinearities and the acceleration terms in these equations as equivalent body forces yields equations amenable to elastic potential solution. Thus, a formulation similar to Papkovitch [23] shows that the Galerkin vector satisfies a nonhomogeneous biharmonic equation and identifies Boussinesq-Papkovitch functions B_0, B_1, B_2 separable into homogeneous (harmonic) and particular components B_{0H}, B_{1H}, B_{2H} and B_{0P}, B_{1P}, B_{2P}, respectively. The former are related to analytic functions $\phi(z)$, $\Psi(z)$ of a complex variable $z = \zeta_1 + i\zeta_2$ (ζ_1, ζ_2 transformed space variables) by $B_{1H} + iB_{2H} = 2(1+\Lambda_0)\,\phi(z)$ and $\partial B_{0H}/\partial\bar{z} = (1+\Lambda_0)\,\overline{\Psi(z)}$, with Λ_0 a constant. Relations of the same type applied to B_{0P}, B_{1P}, B_{2P} define generalized analytic functions $\phi_P(z,\bar{z})$, $\Psi_P(z,\bar{z})$ in the sense treated by Vekua [24]. As a result, the complex displacement $U_1 + iU_2$ can be expressed as a generalization of the usual form [25, p.112], the additional terms being due to $\phi_P(z,\bar{z})$, $\Psi_P(z,\bar{z})$. Traction boundary conditions (5), (6) are treated effectively by a variant of Muskhelishvili's method [25], the difference being that the present complex functions are displacement, not stress, functions. Thus the (usual and generalized) analyticity properties utilized herein follow from the (nonhomogeneous) biharmonic character of the Galerkin vector, rather than that of an Airy stress function; complicated considerations of displacement compatibility are thus avoided by this displacement formulation.

The complex form of boundary conditions (5), (6) is

$$\begin{aligned} &a_1(\zeta_1)\phi'(\zeta_1) + a_2(\zeta_1)\overline{\phi'(\zeta_1)} + \zeta_1\overline{\phi''(\zeta_1)} + \overline{\Psi'(\zeta_1)} = a_3(\zeta_1)\overline{S(\zeta_1)}, \\ &a_2(\zeta_1)\phi'(\zeta_1) + a_1(\zeta_1)\overline{\phi'(\zeta_1)} + \zeta_1\phi''(\zeta_1) + \Psi'(\zeta_1) = a_3(\zeta_1)S(\zeta_1), \end{aligned} \quad (10)$$

with $S(\zeta_1)$ and its complex conjugate $\overline{S(\zeta_1)}$, involving complicated combinations of surface Piola-Kirchhoff stresses and linear and nonlinear displacement gradient and temperature terms, assumed known from previous iterations. Equations (10) are analogous to Muskhelishvili [25], Eqs. (93.3), (93.4), with the added complication that $a_1(\zeta_1)$, $a_2(\zeta_2)$ are surface values of functions that can vary spatially due to thermally-induced material inhomogeneity. However, the functions $w_1(z,\bar{z}) = a_1(z,\bar{z})\phi'(z)$ and $w_2(z,\bar{z}) = a_2(z,\bar{z})\phi'(z)$ satisfy nonhomogeneous Cauchy-Riemann equations $\partial w_k/\partial\bar{z} = A_k w_k$, $A_k = \partial[\log a_k(z,\bar{z})]/\partial\bar{z}$, $(k = 1,2)$, etc. and, hence, are specializations of generalized analytic functions [24]. Consequently, the $w_k(z,\bar{z})$ possess generalized Cauchy kernels $\Omega_{1k}(z,z_s)$, viz.:

$$\Omega_{1k}(z,z_B) = \frac{e^{\omega_{1k}(z,z_B)}}{z_B - z}, \quad (k = 1,2)$$
$$\omega_{1k}(z,z_B) = -\frac{z_B - z}{\pi}\iint_D \frac{A_k(z',\bar{z}')}{(z'-z)(z_B-z')}\,d\zeta_1'd\zeta_2', \quad (11)$$

where z_s denotes a point on the boundary and domain D is the semi-infinite region under consideration. Terms $\zeta_1\overline{\phi''(\zeta_1)}$, $\overline{\Psi'(\zeta_1)}$ in Eqs. (10) are boundary values of functions $z\overline{\phi''(z)}$, $\overline{\Psi'(z)}$ holomorphic in the lower half-plane and $w_1(\zeta_1,\overline{\zeta_1})$, $w_2(\zeta_1,\overline{\zeta_1})$ are boundary values of functions $w_1(z,\bar{z})$, $w_2(z,\bar{z})$ analytic in a generalized sense in the upper and lower half-planes, respectively. Application of the usual Cauchy integral theorem [25] and a generalized Cauchy formula [24, p.175] thus yields relations for $\phi'(z)$, $\Psi'(z)$:

$$\begin{aligned} a_1(z,\bar{z})\phi'(z) = {} & \frac{1}{2\pi i}\int_{-\infty}^{\infty}\frac{a_3(\zeta)\overline{S(\zeta_1)}}{\zeta_1 - z}\,d\zeta_1 \\ & - \frac{1}{2\pi i}\int_{-\infty}^{\infty}\frac{e^{\omega_{11}(z,\zeta_1)} - 1}{\zeta_1 - z}\,a_1(\zeta_1)\phi'(\zeta_1)d\zeta_1 \\ & - \frac{1}{2\pi i}\int_{-\infty}^{\infty}\frac{e^{\omega_{12}(z,\zeta_1)} - 1}{\zeta_1 - z}\,a_2(\zeta_1)\phi'(\zeta_1)d\zeta_1 \end{aligned} \quad (12a)$$

---

[1] $Q^*(\xi_1)$ is the dimensionless surface heat flux, given by the left-hand side of Eq. (7).

$$\Psi'(z) = \frac{1}{2\pi i}\int_{-\infty}^{\infty}\frac{a_3(\zeta_1)S(\zeta_1)}{\zeta_1 - z}\,d\zeta_1 - a_2(z,\bar{z})\phi'(z) - z\phi''(z)$$

$$- \frac{1}{2\pi i}\int_{-\infty}^{\infty}\frac{e^{\omega_{12}(z,\zeta_1)} - 1}{\zeta_1 - z}\,a_2(\zeta_1)\bar{\phi}'(\zeta_1)\,d\zeta_1$$

$$- \frac{1}{2\pi i}\int_{-\infty}^{\infty}\frac{e^{\omega_{11}(z,\zeta_1)} - 1}{\zeta_1 - z}\,a_1(\zeta_1)\overline{\phi'(\zeta_1)}\,d\zeta_1 \qquad (12b)$$

Equations (12) generalize results of Muskhelishvili [25], Eqs. (93.6), (93.7), and demonstrate relevance of an elastic potential solution for nonhomogeneous materials; the first is a linear integral equation, theoretically solvable [17].

NUMERICAL ANALYSIS

General

The complexity of Eqs. (2) - (7) rules out their complete analytical treatment. Thus, their solution must be accomplished numerically, using iteration. To enhance convergence, simultaneous operations with Eqs. (2) - (7) seemed advisable. An iterative finite difference scheme for this purpose idealized the semi-infinite region by a finite rectangular grid, Figure 3, guided by analytical results mentioned above. Detailed application of these results to determine grid size and spacing is described elsewhere [17]. Briefly, however, known exponential decay of temperature in front of the contact ($\xi_1 < 0$) and through the boundary layer thickness facilitates specification of vanishing temperatures and of displacements obtained by linear analysis at the boundaries $\xi_1 = -0.5$ and $\xi_2 = 10\ P_0^{-1/2}$ ($\eta = 10$). Behind the contact ($\xi_1 > 0$), temperature decay is merely algebraic, so choosing $\xi_{1\,max}$ large enough for specification of (approximately) vanishing temperatures there is not feasible.

If Eqs. (2) - (4) were of either parabolic or parabolic-hyperbolic character, formulation as an initial value problem in ξ_1, utilizing forward integration through explicit finite differences, would eliminate the need for boundary values at $\xi_{1\,max}$. The basically elliptic character of Eqs. (2), (3) and the ellipticity of Eq. (4) about $\xi_1 = 0, 1$, $\xi_2 = 0$, together with stability questions inherent in explicit schemes, however, indicated treatment as purely a boundary value problem, using an implicit difference scheme. An effort to limit the number of grid points, dictating a compromise between high grid detail and the magnitude of $\xi_{1\,max}$ used, resulted in $\xi_{1\,max} = 2.5$ and specification there of temperatures and (approximately) vanishing displacement gradients $U_{1,\xi}$, $U_{2,\xi}$ obtained by linear analysis. Boundary conditions (5) - (7) utilized a Hertzian distribution of contact pressure $p(\xi_1)$. The elementary solution for temperatures then involves confluent forms of a hypergeometric function of two variables [17], but the usual result [22] based on a uniform average $p(\xi_1)$ over the contact gives an asymptotically accurate approximation at $\xi_1 = 2.5$.

Finite Difference Form of the Governing Equations

Development of the finite difference approximation of the governing equations followed the form of these equations exhibiting isolated highest derivatives of the dependent variables. Thus, difference operators were applied directly to Eqs. (2) - (7). Use of nonuniform spacings, Figure 3, however, necessitated more general forms of difference operators than are commonly available. Thus, approximation of derivatives with error, order of the grid spacing squared, generally involved 12 grid points, whereas uniform spacing requires nine.

The $3 \times 34 \times 10 = 1020$ difference equations have the matrix form

$$\underset{\sim}{A}(\underset{\sim}{U})\,\underset{\sim}{U} = \underset{\sim}{B}\,; \qquad (13)$$

complicated construction of Eq. (13) is detailed elsewhere [17]. Equation (13) is nonlinear because matrix A is a function of solution vector U, consisting of U_1, U_2, and T' taken successively at each point (I, J)

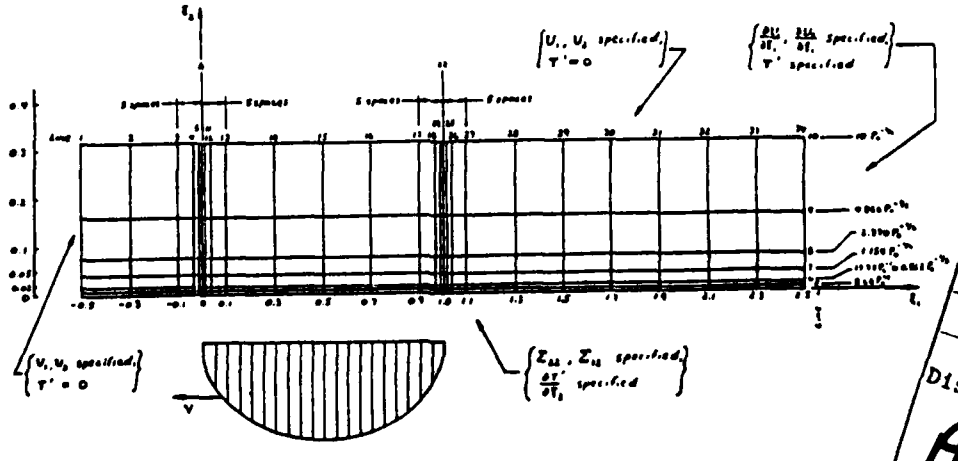

Figure 3 Sample Finite Difference Grid for $P_0 = 1000$, Illustrating Variable Grid Spacing Needed Through the Boundary Layer Thickness and at the Contact Region Leading and Trailing Edges (Spacings smaller than $5P_0^{-1}$ not shown)

left to right in rows 1 through 10. Matrix A is unsymmetric but has banded character, with 41 diagonals on which nonzero elements can occur. Thus, A has $(1020)^2 = 1,040,400$ elements, but only 27,216 are nonzero. Generation of the difference grid, calculation of coefficients for the difference equations, construction of matrix A and vector $\underset{\sim}{B}$ and solution of Eq. (13) were programmed for IBM 3033 computation. NAG [26] subroutines F03AJF and F04APF, designed for large, sparse matrices, were used to triangularize matrix A and solve Eq. (13) by Gaussian elimination. Economy of storage space required identification of only nonzero elements of A and their locations in A. However, nonzero elements occur in four diagonal bands 11, 14, 11, and 5 elements in width, separated by diagonal null bands each 102 zeros in width. Hence, storage requirements for the triangular factors considerably exceed that for the original 27,216 nonzero elements; the actual number of elements generated during triangularization is about 100,000.

Numerical Calculations

Numerical calculations treated a typical contact situation, based on Figures 1 and 3, wherein values of sliding speed (0.8611 m/s), Peclet Number ($P_0 = 1000$), average heat flux (4.43×10^7 N/(m·s)) and thermal parameters were chosen to correspond to those of an earlier study. That study [6] considered temperature-dependent thermal parameters; thus, an envisioned comparison of results obtained therein for SAE 1010 steel with those sought in the present study for the same material offered to clarify the effect of the added nonlinearities. Quadratic variations of λ, μ with T' were used, based on tabulated information [10] for E, ν; similar variations were employed for ν_1, ν_2, ν_3, but only isothermal values for iron [27] could be located as the closest applicable. Although ω_T is a complicated function of V, T' and other factors, information from several sources [17] suggested a temperature dependency of error function type (S-shaped) with ω_T ranging from about 0.115 for 20 - ~ 205°C to about 0.400 above ~ 595°C. Hertzian pressures used corresponded to a contact load of 5.838×10^8 N/(m·s).

Direct searches were made for values of U_1, U_2, T' at the 340 grid points. Ideally, these would lead to solution of nonlinear Eq. (13) by a sequence of Newton-Raphson iterations (Newton's Method in n dimensions, = 1020 for 3 × 340 unknowns), corresponding to successive linear solutions with updating of matrix coefficients. In theory, this process is repeated until convergence is attained, but modification utilizing underrelaxation [28] was found necessary to enhance, or possibly guarantee, convergence. Thus, for iteration k an accepted value of each component U_i of $\underset{\sim}{U}$ is:

$$U_i^{(k)} = \omega_i \bar{U}_i^{(k)} + (1 - \omega_i) U_i^{(k-1)}, \quad i = 1, \ldots, 1020 . \qquad (14)$$

In Eq. (14), the $\bar{U}_i^{(k)}$ are components of the current solution vector and the $U_i^{(k-1)}$ are corresponding components from the previous iteration. The ω_i are relaxation factors, assigned uniform, distinct values ω_1, ω_2, ω_3 for U_1, U_2, T', respectively, variable with k, although variation of the ω_i with location could have been allowed also. Underrelaxation rather than overrelaxation, refers to choices $\omega_i \leq 1$, dictated by solution character; thus, Eq. (14) indicates starting values obtained by interpolation between the results of the previous two iterations.

The above-mentioned searches aimed at establishing the general range of U_1, U_2, T' wherein the true solution $\underset{\sim}{U}$ might lie, subsequent iteration being deferred until convergence in small steps seemed reasonably certain. Progress was limited, however, because large storage requirements for triangularization of A made each linear solution expensive; moreover, setting relaxation factors ω_i by trial and error proved inefficient. Thus, trial starting values of the U_i generated by Eq. (14), if not close to those of the true solution, defined "long" Newton-Raphson tangents (hyperplanes in 1020-degree Euclidian space), giving new values of the U_i from Eq. (13) often far from the starting values. Apparently, convergence speed was dependent on grid point location, seemingly analogous to locally varying degree of stability in forward integration of nonlinear parabolic equations [28, p.325]. Convergence speed was undoubtedly dependent on local grid spacing ratio h_1/h_2, also; although this ratio is, by far, not as critical in boundary value problems as in initial value formulations, large values of h_1/h_2 gave locally anomalous results (mainly for T' central to the contact surface). The searches made indicated that a particular choice of the ω_i offered possible convergence at some locations but divergence at others. Truly effective relaxation must, then, allow for distinct ω_1, ω_2, ω_3 at each of 340 points, but setting all such values by trial and error would be impossible.

A more efficient search technique considers the quantity $\underset{\sim}{A}(\underset{\sim}{U})\underset{\sim}{U} - \underset{\sim}{B}$ of Eq. (13) to represent the gradient $\underset{\sim}{g}(\underset{\sim}{U})$ of some scalar function $f(\underset{\sim}{U})$. Thus, satisfaction of Eq. (13) is equivalent to finding the global minimum of hypersurface $f(\underset{\sim}{U}) = 0$. A quadratic expression for $f(\underset{\sim}{U})$ applies when $\underset{\sim}{A}$ is a symmetric matrix of constants; a more general expression [17] accounts for unsymmetry of A and dependence of A on $\underset{\sim}{U}$. Minimization of $f(\underset{\sim}{U})$ would be difficult. Indeed, starting values for some searches led to $\det[\underset{\sim}{A}(\underset{\sim}{U})] < 0$, indicating $\underset{\sim}{A}(\underset{\sim}{U})$ not everywhere positive definite in the space of $\underset{\sim}{U}$ and $f(\underset{\sim}{U})$ not everywhere convex. Physical realism, however, requires restriction to $\underset{\sim}{U}$ giving positive definite $\underset{\sim}{A}(\underset{\sim}{U})$. Symmetry of $\underset{\sim}{A}(\underset{\sim}{U})$ would guarantee n=1020 mutually orthogonal eigenvectors, "conjugate" with respect to $\underset{\sim}{A}(\underset{\sim}{U})$, spanning the space of $\underset{\sim}{U}$ and providing n = 1020 mutually orthogonal search directions for conjugate gradient minimization[2]. Definiteness of $\underset{\sim}{A}(\underset{\sim}{U})$ ensures that none of the search directions is in the null space of $\underset{\sim}{A}(\underset{\sim}{U})$ and positive definiteness permits quadratic termination (theoretically, in n steps) of the minimization algorithm [29].

Difficulties related to unsymmetry of A can be avoided by utilizing the Hessian matrix

$$\underset{\sim}{H}(\underset{\sim}{U}) = \frac{\partial^2 f}{\partial \underset{\sim}{U} \partial \underset{\sim}{U}} = \frac{\partial \underset{\sim}{g}}{\partial \underset{\sim}{U}} = \underset{\sim}{A}(\underset{\sim}{U}) + \frac{\partial \underset{\sim}{A}}{\partial \underset{\sim}{U}} \underset{\sim}{U} . \qquad (15)$$

Practical calculation of $\partial \underset{\sim}{A}/\partial \underset{\sim}{U}$ for Eq. (15) utilizes linear approximation for a small variation $\Delta \underset{\sim}{U}$:

$$\frac{\partial \underset{\sim}{A}}{\partial \underset{\sim}{U}} \Delta \underset{\sim}{U} \doteq \underset{\sim}{A}(\underset{\sim}{U} + \Delta \underset{\sim}{U}) - \underset{\sim}{A}(\underset{\sim}{U}) . \qquad (16)$$

For independent (scalar) variations ΔU_i of individual U_i, $(\partial \underset{\sim}{A}/\partial \underset{\sim}{U})\Delta \underset{\sim}{U} \rightarrow (\partial \underset{\sim}{A}/\partial U_i)\Delta U_i$ (no sum); thus Eq. (16) gives

$$\frac{\partial \underset{\sim}{A}}{\partial U_i} \doteq \frac{1}{\Delta U_i} [\underset{\sim}{A}(\underset{\sim}{U} + \Delta U_i \underset{\sim}{e}_i) - \underset{\sim}{A}(\underset{\sim}{U})] . \qquad (17)$$

---

[2] Conjugacy in a wider sense for a square, positive definite matrix requires only that the search directions be linearly independent [29, p.153]; these directions may then be orthogonalized by the Gram-Schmidt process [29, p.162]

The term $H(\underset{\sim}{U})$ is symmetric, indicating possible effectiveness of minimizing the quadratic form (with C a scalar constant):

$$S(\underset{\sim}{U}) = \frac{1}{2}\,\underset{\sim}{U}\cdot H(\underset{\sim}{U})\underset{\sim}{U} - \underset{\sim}{B}\cdot\underset{\sim}{U} + C \qquad (18)$$

where $S(\underset{\sim}{U})$ gives a local quadratic, convex fit to $f(\underset{\sim}{U})$. Hence, if a search has located starting values reasonably close to the true solution, locating the global minimum[3] of $S(\underset{\sim}{U})$ approximates that of $f(\underset{\sim}{U})$. An available algorithm [29, pp.165-167] for minimizing $S(\underset{\sim}{U})$ needs further development for a sparse matrix capability and for programming in FORTRAN. Algorithms for storing, transposing and multiplying sparse matrices [30, Chap.3] may be useful also. Fully operational conjugate gradient subroutines available to the author [26,31-33] either lacked a large, sparse matrix capability or required matrix symmetry and positive definiteness.

Although full solution by direct searches was not feasible, the results obtained appear to support a significant influence of nonlinear thermoelastic effects in high temperature situations such as that considered. Thus, the results, although not fully conclusive, implied a maximum surface temperature (at $\xi_1 = 0.8$) of roughly 780°C ($T' = 2.6$), contrasting with about 535°C considering nonlinear thermal effects along [16] and about 615°C from elementary theory [6]. Similarly, a maximum surface outward normal displacement of roughly 0.003 in. was implied. (Corresponding strains as large as roughly 0.01 in./in. indicated some possible yielding for the steel considered.) Equations (18), (19) show that displacement gradient effects begin to dominate contributions from λ, μ when $|A_4 U_{1,1}|$, $|A_5 U_{2,2}|$, $|A_4 U_{2,2}|$, $|A_5 U_{1,1}| = O(\lambda + 2\mu)$, $|A_3 U_{1,1}|$, $|A_3 U_{2,2}| = O(\lambda + \mu)$, $|A_1 U_{1,1}|$, $|A_1 U_{2,2}| = O(\mu)$, etc. For the steel considered these criteria reduce to $|U_{1,1}| = O(0.006)$, $|U_{2,2}| = O(0.02)$, although lack of high-temperature data for ν_1, ν_2, ν_3 permits comparisons for only isothermal parameters. Occurrence of locally negative squares of wave speeds, Eqs.(8), may lead to failure of matrix A to be positive definite, a condition presumably related to $\det(A) < 0$ noted for some searches.

ACKNOWLEDGEMENT

The author wishes to thank Dr. Frederick F. Ling for frequent encouragement, guidance, and helpful discussions. Work was supported in part by the Office of Naval Research and the Army Research Office under Contracts N00014-80-C-0253 and DAAG 29-79-C-0204, respectively, with Rensselaer Polytechnic Institute.

REFERENCES

1. Barber, J.R., "Thermoelastic Instabilities in the Sliding of Conforming Solids," Proceedings of the Royal Society, Series A, Vol.312, 1969, pp.381-394.

2. Dow, T.A. and Stockwell, R.D., "Experimental Verification of Thermoelastic Instabilities in Sliding Contact," Journal of Lubrication Technology, Trans. ASME, Series F, Vol.99, 1977, pp.359-364.

3. Ling, F.F. and Simkins, T.E., "Measurement of Pointwise Juncture Condition of Temperature at the Interface of Two Bodies in Sliding Contact," Journal of Basic Engineering, Trans. ASME, Series D, Vol.85, 1963, pp.481-487.

[3] Surfaces $S_1^* =$ constant are ellipsoids with principal axes $(2S_1^*/\lambda_i)^{1/2}$, $i = 1, \ldots, n$, λ_i being eigenvalues of $H(\underset{\sim}{U})$. The more nearly equal the λ_i, the nearer the approach is to spheroids and the more rapid is convergence [30, pp.216-218].

4. Boley, B.A. and Weiner, J.H., Theory of Thermal Stresses, Wiley, New York, 1960, pp.42-44.

5. Dillon, O.W., "Temperature Generated in Aluminum Rods Undergoing Torsional Oscillations," Journal of Applied Physics, Vol.33, 1962, pp.3160-3165.

6. Ling, F.F. and Rice, J.S., "Surface Temperature with Temperature-Dependent Thermal Properties," Trans. ASLE, Vol.9, 1966, pp.195-201.

7. Farren, W.S. and Taylor, G.I., "The Heat Developed During Plastic Extension of Metals," Proceedings of the Royal Society, Series A, Vol.107, 1925, pp.422-451.

8. Touloukian, Y.S. (Editor), Thermophysical Properties of High Temperature Solid Materials, MacMillan/Pergamon, New York, 1967.

9. Lucks, C.F. and Deem, H.W., "Thermal Properties of Thirteen Metals," ASTM Special Technical Publication No.227, ASTM, Philadelphia, Pennsylvania, 1958, pp.1-29.

10. Garofalo, F., Malenock, P.R. and Smith, G.V., "The Influence of Temperature on the Elastic Constants of Some Common Steels," Symposium on Determination of Elastic Constants, ASTM Special Technical Publication No.129, ASTM, Philadelphia, Pennsylvania, 1952, pp.1-30.

11. Ling, F.F., "A Quasi-Iterative Method for Computing Interface Temperature Distributions," Zeitschrift für Angewandte Math. und Physik, Vol.10, 1959, pp.461-479.

12. Stoker, J.J., Nonlinear Vibrations, Interscience, New York, 1950.

13. Truesdell, C. and Toupin, R., "The Classical Field Theories," Handbuch der Physik, Vol.III/1, Springer-Verlag, Berlin, 1960.

14. Truesdell, C. and Noll, W., "The Nonlinear Field Theories of Mechanics," Handbuch der Physik, Vol.III/3, Springer-Verlag, Berlin, 1965.

15. Chadwick, P. and Sect, L.T.C., "Second-Order Thermoelasticity Theory for Isotropic and Transversely Isotropic Materials, Trends in Elasticity and Thermoelasticity, Wolters-Noordhoff, Groningen, 1971, pp.27-57.

16. Courant, R. and Hilbert, D., Methods of Mathematical Physics, Vol.2, Interscience, New York, 1962, p.580.

17. Pitkin, J.M., "Nonlinear Thermoelastic Effects in Surface Mechanics," Thesis, Rensselaer Polytechnic Institute, December 1981.

18. Knowles, J.K. and Sternberg, E., "On the Failure of Ellipticity of the Equations for Finite Elastostatic Plane Strain," Archive for Rational Mechanics and Analysis, Vol.63, 1977, pp.321-336.

19. Knowles, J.K. and Sternberg, E., "On the Failure of Ellipticity and the Emergence of Discontinuous Deformation Gradients in Plane Finite Elastostatics," Journal of Elasticity, Vol.8, 1978, pp.329-379.

20. Messiter, A.F., "Boundary-Layer Flow Near the Trailing Edge of a Flat Plate," SIAM Journal of Applied Mathematics, Vol.18, 1970, pp.241-257.

21. Stewartson, K., "On the Flow Near the Trailing Edge of a Flat Plate," - I, Proceedings of the Royal Society, Series A, Vol.306, 1968, pp.275-290; - II, Mathematika, Vol.16, 1969, pp.106-121.

22. Carslaw, H.S. and Jaeger, J.C., Conduction of Heat in Solids, Oxford, London, Second Edition, 1959.

23. Papkovitch, P.F., "Solution Générale des Équations Differentielles Fondamentales d'Élasticité, Exprimée par Trois Fonctions Harmoniques," Comptes Rendus de l'Académie des Sciences, Paris, Vol.195, 1932, pp.513-515. Also, "Expressions Générales des Composantes des Tensions, ne Renfermant comme Fonctions Arbitraires que des Fonctions Harmoniques," ibid., pp.754-756.

24. Vekua, I.N., Generalized Analytic Functions (1959), Porgamon/Addison-Wesley, Reading, 1962.

25. Muskhelishvili, N.I., Some Basic Problems of the Mathematical Theory of Elasticity, Fourth Edition (1954), Noordhoff, Groningen, 1963.
26. Numerical Algorithms Group (NAG), Oxford, FORTRAN Subroutine Library, Vol.5, May 1977.
27. Seeger, A., Discussion of Foux, A., "An Experimental Investigation of the Poynting Effect," IUTAM Symposium on Second Order Effects in Elasticity, Plasticity, and Fluid Dynamics, Pergamon/MacMillan, New York, 1964, pp.228-251.
28. Ames, W.F., Nonlinear Partial Differential Equations in Engineering, Prentice-Hall, Englewood Cliffs, 1961.
29. Nash, J.C., Compact Numerical Methods for Computers: Linear Algebra and Function Minimisation, Wiley, New York, 1979.
30. Jennings, A., Matrix Computation for Engineers and Scientists, Wiley/Interscience, New York, 1977.
31. International Mathematical and Statistical Libraries (IMSL), Houston, FORTRAN Subroutine Library, 1980.
32. Harwell Numerical Analysis, Computer Sciences and System Division of UKAERA, Oxfordshire, FORTRAN Subroutine Library, 1980.
33. Argonne National Laboratory, Applied Mathematics Division, Chicago, LINPACK FORTRAN Subroutine Library, 1981.

APPENDIX - COEFFICIENT TERMS FOR EQS. (2) - (6)

$$
\begin{aligned}
\rho_o v_{111}^2 &= (\lambda + 2\mu) + A_4 U_{1,1} + A_5 U_{2,2} - \beta T' ,\\
\rho_o v_{222}^2 &= (\lambda + 2\mu) + A_4 U_{2,2} + A_5 U_{1,1} - \beta T' ,\\
\rho_o v_{212}^2 &= (\lambda + \mu) + A_3 U_{1,1} + A_3 U_{2,2} ,\\
\rho_o v_{122}^2 &= \mu + A_1 U_{1,1} + A_1 U_{2,2} - \beta T' ,\\
\rho_o v_{211}^2 &= A_2 U_{1,2} + A_1 U_{2,1} ,\\
\rho_o v_{112}^2 &= A_1 U_{1,2} + A_2 U_{2,1} ,\\
\rho_o v_{113}^2 &= (\beta T')' + (\lambda + 2\mu - \beta T')' U_{1,1} + \lambda' U_{2,2} ,\\
\rho_o v_{123}^2 &= (\mu - \beta T')' U_{1,2} + \mu' U_{2,1} ,\\
\rho_o v_{213}^2 &= \mu' U_{1,2} + (\mu - \beta T')' U_{2,1} ,\\
\rho_o v_{223}^2 &= (\beta T')' + \lambda' U_{1,1} + (\lambda + 2\mu - \beta T')' U_{2,2} ,\\
\rho_o \hat{v}_{311}^2 &= [(\beta T')' - (\lambda - 2\mu)' E_{11} - \lambda' E_{22}](1 + U_{1,1}) \\
&\quad - 2\mu' E_{12} U_{1,2} ,\\
\rho_o \hat{v}_{312}^2 &= [(\beta T')' - \lambda' E_{11} - (\lambda + 2\mu)' E_{22}] U_{1,2} \\
&\quad - 2\mu' E_{12}(1 + U_{1,1}) ,\\
\rho_o \hat{v}_{411}^2 &= [(\beta T')' - (\lambda + 2\mu)' E_{11} - \lambda' E_{22}] U_{2,1} \\
&\quad - 2\mu' E_{12}(1 + U_{2,2}) ,\\
\rho_o \hat{v}_{412}^2 &= [(\beta T')' - \lambda' E_{11} - (\lambda + 2\mu)' E_{22}](1 + U_{2,2}) \\
&\quad - 2\mu' E_{12} U_{2,1} ,\\
\rho_o \hat{v}_1^2 &= (\beta T')'(E_{11} + E_{22}) , \qquad v_T^2 = c_o T_o ,\\
&\{v_{311}^2, v_{312}^2, v_{411}^2, v_{412}^2, v_1^2\} \\
&\quad = \frac{1 + T'}{g} \{\hat{v}_{311}^2, \hat{v}_{312}^2 \hat{v}_{411}^2, \hat{v}_{412}^2, \hat{v}_1^2\} ,
\end{aligned}
\tag{19}
$$

$$
\begin{aligned}
P_{N11} &= \lambda + A_5 U_{1,1} ,\\
P_{N22} &= (\lambda + 2\mu - \beta T') + A_5 U_{1,1} + (2\mu + A_4/2) U_{2,2} ,\\
P_{N12} &= \tfrac{1}{2} A_1 U_{1,2} + (\mu + A_2/2) U_{2,1} ,\\
P_{N21} &= (\mu + A_2/2) U_{1,2} + \tfrac{1}{2} A_1 U_{2,1} ,\\
P_{S12} &= (\mu - \beta T') + A_1 (U_{1,1} + U_{2,2}) ,\\
P_{S21} &= \mu + (2\mu + A_2)(U_{1,1} + U_{2,2}) ,
\end{aligned}
\tag{20}
$$

$$
\begin{aligned}
A_1 &= \lambda + 2\mu + \nu_2 + 2\nu_3 ,\\
A_2 &= \mu + \nu_2 + 2\nu_3 ,\\
A_3 &= \lambda + \mu + \nu_1 + 3\nu_2 + 2\nu_3 ,\\
A_4 &= 2A_1 + A_2 + A_3 ,\\
A_5 &= A_3 - A_2 .
\end{aligned}
\tag{21}
$$

ME

8